RESEARCH PAPER

The antimalarial drugs quinine, chloroquine and mefloquine are antagonists at 5-HT$_3$ receptors

AJ Thompson, M Lochner and SCR Lummis

Department of Biochemistry, University of Cambridge, Cambridge, UK

Background and Purpose: The antimalarial compounds quinine, chloroquine and mefloquine affect the electrophysiological properties of Cys-loop receptors and have structural similarities to 5-HT$_3$ receptor antagonists. They may therefore act at 5-HT$_3$ receptors.

Experimental Approach: The effects of quinine, chloroquine and mefloquine on electrophysiological and ligand binding properties of 5-HT$_{3A}$ receptors expressed in HEK 293 cells and *Xenopus* oocytes were examined. The compounds were also docked into models of the binding site.

Key Results: 5-HT$_3$ responses were blocked with IC_{50} values of 13.4 µM, 11.8 µM and 9.36 µM for quinine, chloroquine and mefloquine. Schild plots indicated quinine and chloroquine behaved competitively with pA_2 values of 4.92 ($K_B = 12.0$ µM) and 4.97 ($K_B = 16.4$ µM). Mefloquine displayed weakly voltage-dependent, non-competitive inhibition consistent with channel block. On and off rates for quinine and chloroquine indicated a simple bimolecular reaction scheme. Quinine, chloroquine and mefloquine displaced [^{3}H]granisetron with K_i values of 15.0, 24.2 and 35.7 µM. Docking of quinine into a homology model of the 5-HT$_3$ receptor binding site located the tertiary ammonium between W183 and Y234, and the quinoline ring towards the membrane, stabilised by a hydrogen bond with E129. For chloroquine, the quinoline ring was positioned between W183 and Y234 and the tertiary ammonium stabilised by interactions with F226.

Conclusions and Implications: This study shows that quinine and chloroquine competitively inhibit 5-HT$_3$ receptors, while mefloquine inhibits predominantly non-competitively. Both quinine and chloroquine can be docked into a receptor binding site model, consistent with their structural homology to 5-HT$_3$ receptor antagonists.

British Journal of Pharmacology (2007) **151**, 666–677; doi:10.1038/sj.bjp.0707238; published online 14 May 2007

Introduction

For most of the last century drugs such as quinine, chloroquine and mefloquine (Lariam) have provided a safe, cheap and effective method of controlling malaria. The antimalarial properties of these compounds are thought to be a consequence of inhibiting parasite growth within infected erythrocytes (Bray *et al.*, 2005; Uhlemann *et al.*, 2005). However, there are a growing number of clinical reports that show these drugs may also have neurological side effects, including paranoia, anxiety and depression. Emerging experimental evidence supports the hypothesis that these compounds adversely affect transmission at both neuromuscular junctions and synapses. For example, quinine has been shown to reduce the quantal content of miniature end-plate potentials at neuromuscular junctions and cause an open and closed channel block of postsynaptic nicotinic acetylcholine (nACh) receptors (Sieb *et al.*, 1996). Block of α9α10 nACh receptors by chloroquine has shown that this compound acts as a competitive inhibitor while quinine displays a mixed competitive/noncompetitive behaviour (Ballestero *et al.*, 2005). As 5-HT$_3$ receptors are closely related to nACh receptors, it is possible that these antimalarial compounds also affect 5-hydroxytryptaminergic neurotransmission. Furthermore, pharmacophore models of 5-HT$_3$ agonists and antagonists have structural features that are shared by quinine, chloroquine and mefloquine, suggesting that these compounds may interact with the 5-HT$_3$-binding site.

5-HT$_3$ receptors are members of the Cys-loop family of ligand-gated ion channels that also include nACh, glycine and GABA$_A$ receptors. These receptors are membrane proteins composed of five symmetrically arranged subunits that surround a central ion-conducting pore. To date, five 5-HT$_3$ receptor subunits (A–E) have been identified, although

Correspondence: Dr S Lummis, Department of Biochemistry, Tennis Court Road, Cambridge CB2 1QW, UK.
E-mail: sl120@cam.ac.uk

Antimalarial drugs inhibit 5-HT$_3$ receptors
AJ Thompson et al
667

only homomeric 5-HT$_{3A}$ or heteromeric 5-HT$_{3AB}$ subunit complexes have been functionally expressed and characterized (Davies et al., 1999; Niesler et al., 2003). Each subunit consists of an extracellular, a transmembrane and an intracellular domain. The extracellular domain is responsible for ligand binding. The binding site is located at the interface of two adjacent subunits and is formed by the convergence of three loops (A–C) from the principal subunit and another three loops (D–F) from the complementary subunit (Reeves and Lummis, 2002). Molecular details of the binding pocket have been extrapolated from the structure of the acetylcholine-binding protein (AChBP), which is homologous to the extracellular domain of Cys-loop receptors, and a range of amino-acid residues that are important for agonist and antagonist binding have been identified (see for example Thompson et al., 2006b). 5-HT$_3$ receptors are present in the central and peripheral nervous system where activation results in membrane depolarization under physiological conditions. Postsynaptic activation contributes to fast excitatory transmission and presynaptic receptors modulate the release of various neurotransmitters such as dopamine and GABA (Thompson et al., 2006b). Consequently, changes in the proper functioning of these receptors could have a wide-ranging impact on neurological function and may partially explain some of the reported side effects associated with malarial prophylaxis.

Using recombinant expressed receptors, we show that quinine, chloroquine and mefloquine inhibit 5-HT$_3$ receptor-mediated currents and binding of the radiolabelled 5-HT$_3$ receptor antagonist, [3H]granisetron. A mechanism for the effects of each compound is proposed.

Materials and methods

Cell culture and oocyte maintenance
Human embryonic kidney (HEK)-293 cells were maintained in DMEM/F12 (Dulbecco's modified Eagle's medium/nutrient mix F12 (1:1)) with GlutaMAX I containing 10% fetal calf serum at 37°C and 7% CO$_2$ in a humidified atmosphere. Xenopus laevis oocyte-positive females were purchased from NASCO (Fort Atkinson, WI, USA) and maintained according to standard methods (Goldin, 1992). Harvested stage V–VI Xenopus oocytes were washed in six changes of ND96 (96 mM NaCl, 2 mM KCl, 1 mM MgCl$_2$, 1.8 mM CaCl$_2$ and 5 mM HEPES, pH 7.5), defolliculated in 1.5 mg ml^{-1} collagenase Type 1A for approximately 2 h, washed again in a further six changes of ND96 and stored in ND96 containing 2.5 mM sodium pyruvate, 50 mM gentamycin and 0.7 mM theophylline.

Receptor expression
Mouse 5-HT$_{3A}$ (accession number: AY605711) subunit cDNA was cloned into pGEMHE for oocyte expression (Liman et al., 1992). cRNA was in vitro-transcribed from linearized (NheI) plasmid cDNA template using the mMessage mMachine T7 Transcription kit (Ambion, Austin, TX, USA). Stage V and VI oocytes were injected with 100–700 ng cRNA and recorded from 1 to 4 days post-injection. For expression in HEK-293 cells, 5-HT$_{3A}$ receptor subunit cDNA was cloned into pcDNA3.1 (Invitrogen Ltd, Paisley, UK). Cells were transfected using calcium phosphate precipitation at 80–90% confluency (Jordan et al., 1996). After transfection cells were incubated for 3–4 days before assay.

Radioligand binding
This was undertaken in HEK-293 cells, which provide an established and robust method of studying ligand binding. Methods were as described previously (Lummis et al., 1993), with minor modifications. Briefly, transfected HEK-293 cells were washed twice with phosphate-buffered saline (PBS) at room temperature and scraped into 1 ml of ice-cold HEPES buffer (10 mM, pH 7.4) containing the following proteinase inhibitors (PIs): 1 mM EDTA, 50 μg ml^{-1} soybean trypsin inhibitor, 50 μg/ml bacitracin and 0.1 mM phenylmethylsulphonyl fluoride. After thawing, they were washed with HEPES buffer, resuspended, and 50 μg of cell membranes incubated in 0.5 ml HEPES buffer containing 1 nM [3H]granisetron ($\sim K_d$) in the presence or absence of quinine, chloroquine or mefloquine (0.5 μM to 2 mM). Competition binding (16 point) was performed on at least four separate plates of transfected cells. Nonspecific binding was determined using 10 μM quipazine. Reactions were incubated for at least 1 h at 4°C and terminated by vacuum filtration using a Brandel cell harvester onto GF/B filters presoaked in 0.3% polyethyleneimine. Radioactivity was determined by scintillation counting using a Beckman LS6000SC (Fullerton, CA, USA). Competition binding data were analysed by iterative curve fitting (GraphPad Prism v3.02, GraphPad Software, San Diego, CA, USA), according to the equation:

$$y = B_{min} + \frac{B_{max} - B_{min}}{1 + 10^{[L] - \log IC_{50}}} \qquad (1)$$

where B_{min} is the lowest specific binding, B_{max} is the maximum specific binding, $[L]$ is the concentration of competing ligand and IC_{50} is the concentration of competing ligand that blocks half of the specific bound radioligand. K_i values were estimated from IC_{50} values using the Cheng–Prusoff equation:

$$K_i = \frac{IC_{50}}{1 + [L]/K_d} \qquad (2)$$

where K_i is the equilibrium dissociation constant for binding of the unlabelled antagonist, $[L]$ is the concentration of radioligand and K_d is the equilibrium dissociation constant of the radioligand. Values are presented as mean$\pm$s.e.m.

Electrophysiology
Electrophysiological experiments were performed in Xenopus oocytes that express 5-HT$_3$ receptors better than HEK-293 cells, resulting in larger currents that are more accurate for inhibition studies. Using two electrode voltage clamp, oocytes were routinely clamped at −60 mV (unless stated) using an OC-725 amplifier (Warner Instruments, Hamden, CT, USA), Digidata 1322A and the Strathclyde Electrophysiology Software Package (Strathclyde Institute of Pharmacy
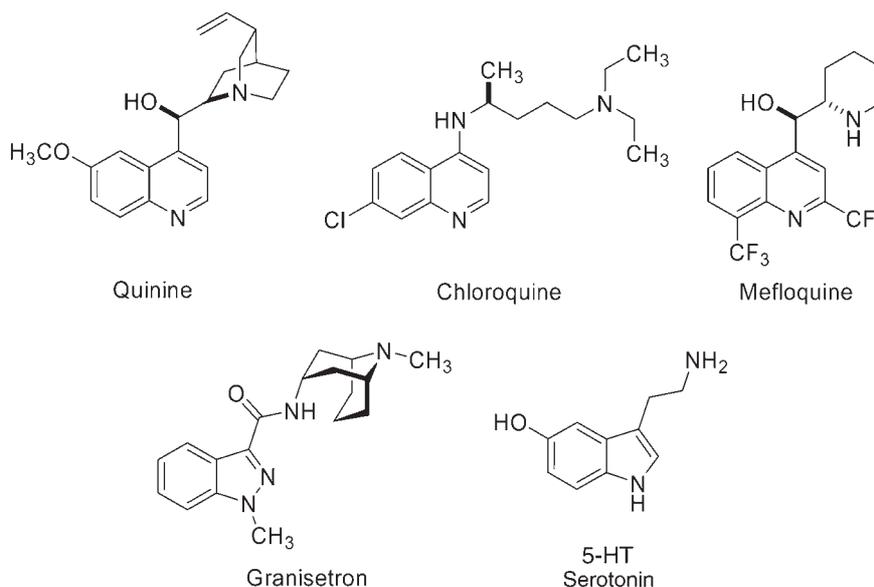
Antimalarial drugs inhibit 5-HT₃ receptors
AJ Thompson *et al*
668

Figure 1 Structural formulae of quinine, chloroquine and mefloquine. An agonist (5-HT) and competitive antagonist (granisetron) have been included for comparison.

& Biomedical Sciences, University of Strathclyde, UK; http://www.strath.ac.uk/sipbs/). Currents were filtered at a frequency of 1 kHz. Leak current was always < 100 nA. Microelectrodes were fabricated from borosilicate glass (GC120TF-10, Harvard Apparatus, Edenbridge, Kent, UK) using a two-stage horizontal pull (Sutter P-87, Novato, CA, USA) and filled with 3 M KCl. Pipette resistances ranged from 0.5 to 1.5 MΩ. Oocytes were perfused with saline at a rate of 15 ml min^{-1}. Drug application was via a simple gravity-fed system calibrated to run at the same rate. Extracellular saline contained (mM), 96 NaCl, 2 KCl, 1 MgCl₂ and 5 HEPES; pH 7.4 with NaOH.

Data analysis
Analysis and curve fitting were performed using Prism. Concentration–response data for each oocyte were normalized to the maximum current for that oocyte. For inhibition curves, antagonists were either co-applied with 5-HT or were preapplied for 25 s and then immediately co-applied. The mean and s.e.m. for a series of oocytes were plotted against agonist or antagonist concentration and iteratively fitted to the following equation:

$$y = I_{min} + \frac{I_{max} - I_{min}}{1 + 10^{\log(EC_{50} - [L])^{n_H}}} \qquad (3)$$

where I_{min} is the baseline current, I_{max} is the peak current evoked by agonist, EC_{50} is the concentration of agonist needed to evoke a half-maximal response, $[L]$ is the antagonist concentration and n_H is the Hill slope. K_b was estimated from IC_{50} values using the Cheng–Prusoff equation with the modification by Leff and Dougall (1993).

$$K_b = \frac{IC_{50}}{((2 + ([L]/[EC_{50}])^{n_H})^{1/n_H}) - 1} \qquad (4)$$

where K_b is the dissociation constant of the competing drug, IC_{50} is the concentration of antagonist required to halve the

maximal response, $[L]$ is the agonist concentration, $[EC_{50}]$ is the agonist EC_{50} and n_H is the Hill slope of the agonist. Analysis of competitive inhibition was performed by Schild plot (Arunlakshana and Schild, 1959) according to the following equation:

$$\log[(EC_{50}'/EC_{50}) - 1] = \log[L] - \log K_B \qquad (5)$$

where EC_{50}' and EC_{50} are values in the presence and absence of antagonist (dose ratio), $[L]$ is the concentration of antagonist and K_B is the equilibrium dissociation constant for the antagonist receptor interaction. Further analysis was performed using the Gaddum–Schild equation (slope = 1) as recommended by (Neubig *et al.*, 2003)

$$pEC_{50} = -\log([L] + 10^{-pA_2}) - \log C \qquad (6)$$

where pEC_{50} is the negative logarithm of the agonist EC_{50}, $[L]$ is the antagonist concentration, $\log C$ is a constant and pA_2 is the negative logarithm of the antagonist concentration needed to double the concentration of agonist required, to elicit a response that is comparable to the original response in the absence of antagonist. pA_2 is equal to the negative logarithm of K_B when the slope of the Schild plot is exactly 1.

Rate constants for the onset and recovery from antagonist inhibition were analysed as follows. A simple bimolecular binding scheme for receptor and ligand can be represented as

$$L + R \underset{k_{-1}}{\overset{k_{+1}}{\rightleftharpoons}} LR \qquad (7)$$

where L is ligand concentration, R is receptor concentration, LR is the bound receptor and k_{+1} and k_{-1} are the microscopic association and dissociation rate constants. In a simple scheme such as this, the apparent equilibrium dissociation constant (K_d) is equal to the ratio of dissociation
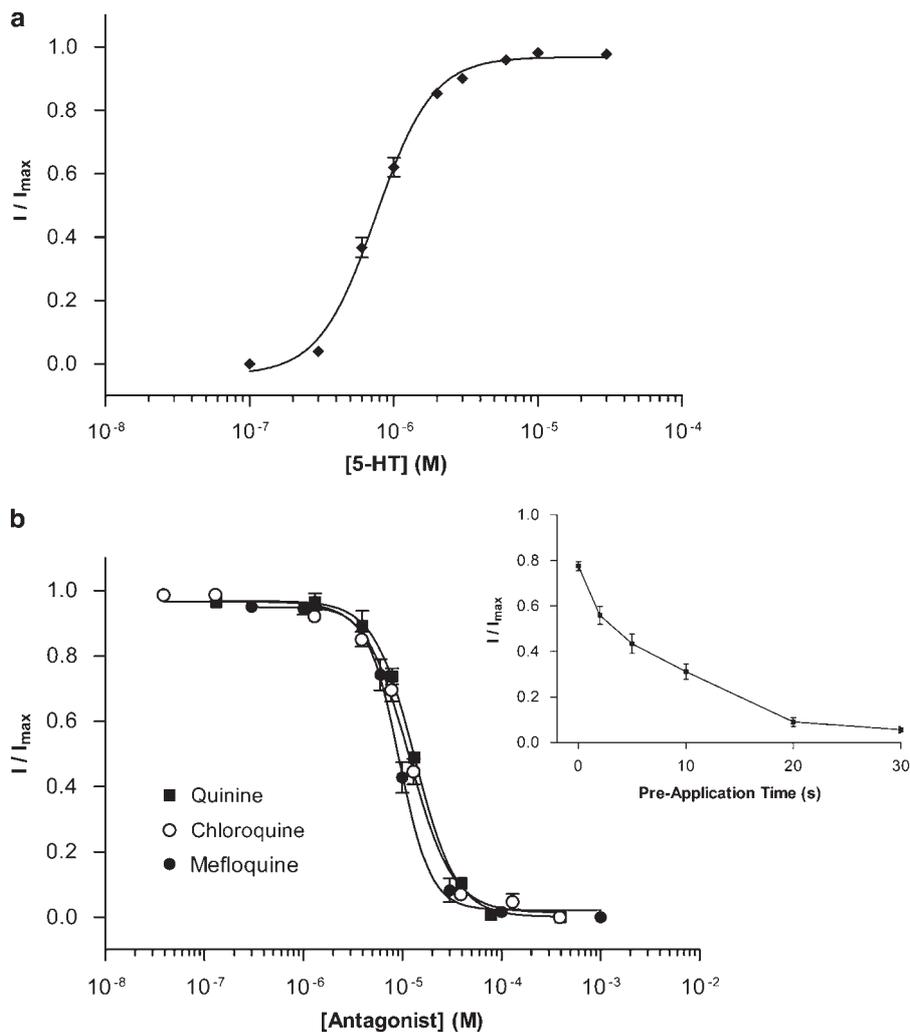
Antimalarial drugs inhibit 5-HT$_3$ receptors
AJ Thompson et al
669

Figure 2 Concentration–response (**a**) and dose–inhibition (**b**) curves for 5-HT$_3$ receptor currents. Inhibition was measured in the presence of 0.75 μM 5-HT (EC$_{50}$). Quinine and chloroquine inhibition were recorded during the co-application of 5-HT. Mefloquine was pre-applied for 25 s and was immediately followed by co-application with 5-HT. Inset: inhibition versus pre-application time for 30 μM mefloquine ($n = 7$). The data are normalized to the maximum response in each oocyte and represented as the mean $\pm$ s.e.m. for a series of oocytes. Parameters derived from these curves can be seen in Table 1.

Table 1 Parameters derived from inhibition curves

	log IC$_{50}$ (μM)	IC$_{50}$ (μM)	n$_H$	n
Quinine	-4.87 ± 0.02	13.4	-2.09 ± 0.18	12
Chloroquine	-4.93 ± 0.02	11.8	-1.90 ± 0.39	14
Mefloquine	-5.03 ± 0.02	9.36	-2.08 ± 0.18	13

to association rate constants, such that

$$K_{d} = \frac{k_{-1}}{k_{+1}} \qquad (8)$$

According to a one site-binding model of the type shown, the rates of onset and recovery of an antagonist response can be used to estimate k_{+1} and k_{-1}

$$1/\tau_{off} = k_{-1} \qquad (9)$$

and

$$1/\tau_{on} = k_{+1}[L] + k_{-1} \qquad (10)$$

where τ_{on} refers to the rate of onset of inhibition, τ_{off} refers to recovery from inhibition and [L] is antagonist concentration.

Modelling and antagonist docking
The protein sequence of the extracellular domain of the mouse 5-HT$_{3A}$ receptor subunit (accession number: Q6J1J7) was co-aligned with the sequence of AChBP from *Lymnaea stagnalis* (accession number: P58154) using FUGUE (Shi *et al.*, 2001). A three-dimensional homology model was generated using MODELLER 6v2 (Sali and Blundell, 1993) based on the crystal structure of AChBP at 2.7 Å resolution (PDB ID: 1I9B). The pentamer was generated by superimposing a 5-HT$_3$ subunit onto each protomer of AChBP and was then energy minimized using the force field implemented in MODELLER

6v2. The best model was selected after Ramachandran plot analysis of all the generated models.

The three-dimensional structures of quinine and chloroquine were extracted from the Cambridge Structural Database (reference codes KAMDAD and CLQUON01, respectively). Protonated forms of both molecules were constructed in Chem3D Ultra 7.0 (CambridgeSoft, Cambridge, UK) based on the crystal structures, and energy minimized using the MM2 force field. Figure 1 shows the structural formulae of these compounds.

Docking of the protonated ligands into the 5-HT$_3$ receptor homology model was carried out using GOLD 3.0 (The Cambridge Crystallographic Data Centre, Cambridge, UK). The binding site was defined using the C$_{\varepsilon2}$ atom of W183, the C$_\zeta$ atom of Y234 or the C$_\zeta$ atom of Y153, with a binding site radius of 7 Å for quinine and 10 Å for chloroquine. The amino-acid residues were chosen based on the preferred binding site models of Reeves *et al.* (2003) and Thompson *et al.* (2005). Ten genetic algorithm runs were performed on each docking exercise, giving a total of 30 solutions for each antagonist. The structures were analysed using the implemented GoldScore fitness function.

Materials

All cell culture reagents were obtained from Gibco BRL (Paisley, UK), except fetal calf serum which was from Labtech International (Ringmer, UK). [^{3}H]granisetron (63.5 Ci mmol^{-1}) was from PerkinElmer (Boston, MA, USA). Quinine and chloroquine were from Sigma-Aldrich Co. Ltd (Poole, Dorset, UK). Mefloquine-HCl was provided by CilagAG. All other reagents were of the highest obtainable grade.

Results

Effects of antimalarial compounds on 5-HT$_3$ receptor-mediated currents

Application of 5-HT to *Xenopus* oocytes expressing 5-HT$_3$ receptors produced concentration-dependent, rapidly activating, inward currents that desensitized over the time course of the application. Plotting current amplitude against a series of 5-HT concentrations allowed the data to be fitted with Equation 3, from which a log EC$_{50}$ of -6.12 ± 0.02 (EC$_{50} = 0.75 \mu$M) and Hill slope of 2.21 ± 0.23 were calculated (Figure 2a, $n = 12$). These responses were completely and reversibly inhibited by the antagonists d-tubocurarine and granisetron (100 nM, data not shown).

Inhibition of the 0.75μM 5-HT-induced response was observed in the presence of quinine, chloroquine or mefloquine, but application of antagonists alone did not elicit a response (Figure 2b, Table 1). The inhibition was fully reversible after 3 min of washing. Inhibition was unaltered by pre-application of quinine or chloroquine, but an increase in potency was seen for mefloquine with no significant change in the level of inhibition after 20 s of pre-application (Figure 2b, inset). In the continued presence of 5-HT, removal of all these the drugs resulted in the reemergence of the current (Figure 3). IC$_{50}$ values for the three
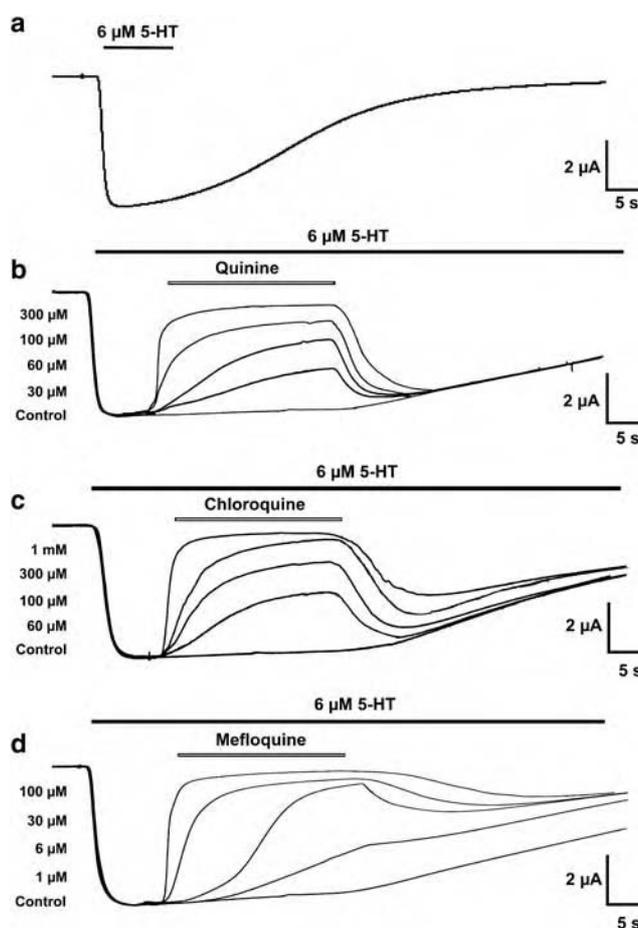

Figure 3 Quinine, chloroquine and mefloquine inhibition of the 5-HT$_3$ receptor. A typical response in the presence of 6μM 5-HT alone (**a**) and inhibition of the 6μM 5-HT response by quinine (**b**), chloroquine (**c**) and mefloquine (**d**). Note that the 5-HT response fully recovers following the removal of quinine. For chloroquine a similar observation was made at lower ($<100 \mu$M, that is within the range of the dose–inhibition curve) concentrations of the antagonist. In contrast, mefloquine inhibition persisted after its application had ceased.

compounds were similar with a rank order of potency of mefloquine > chloroquine > quinine. The data from these experiments were used in the modified Cheng–Prusoff (Equation 4) and yielded K_b values of 37.4 and 32.8μM for quinine and chloroquine. A K_b estimate for mefloquine could not be accurately determined as further observations indicated that this compound displayed a noncompetitive behaviour (Leff and Dougall, 1993).

Mechanism of block

Increasing the concentrations of quinine (50, 100, 160 and 300μM) and chloroquine (30, 80, 100, 150 and 300μM) caused parallel rightward shifts in the 5-HT concentration–response curves, with no change in the maximal response (Figure 4a and b, Table 2), indicating competitive inhibition. Schild plots supported this finding (Equation 5, Figure 4a and b inset), yielding gradients close to 1 (0.99 and 0.96) and pA$_2$ values of 4.92 (K_B, 12.0μM) and 4.79 (K_B, 16.4μM) for
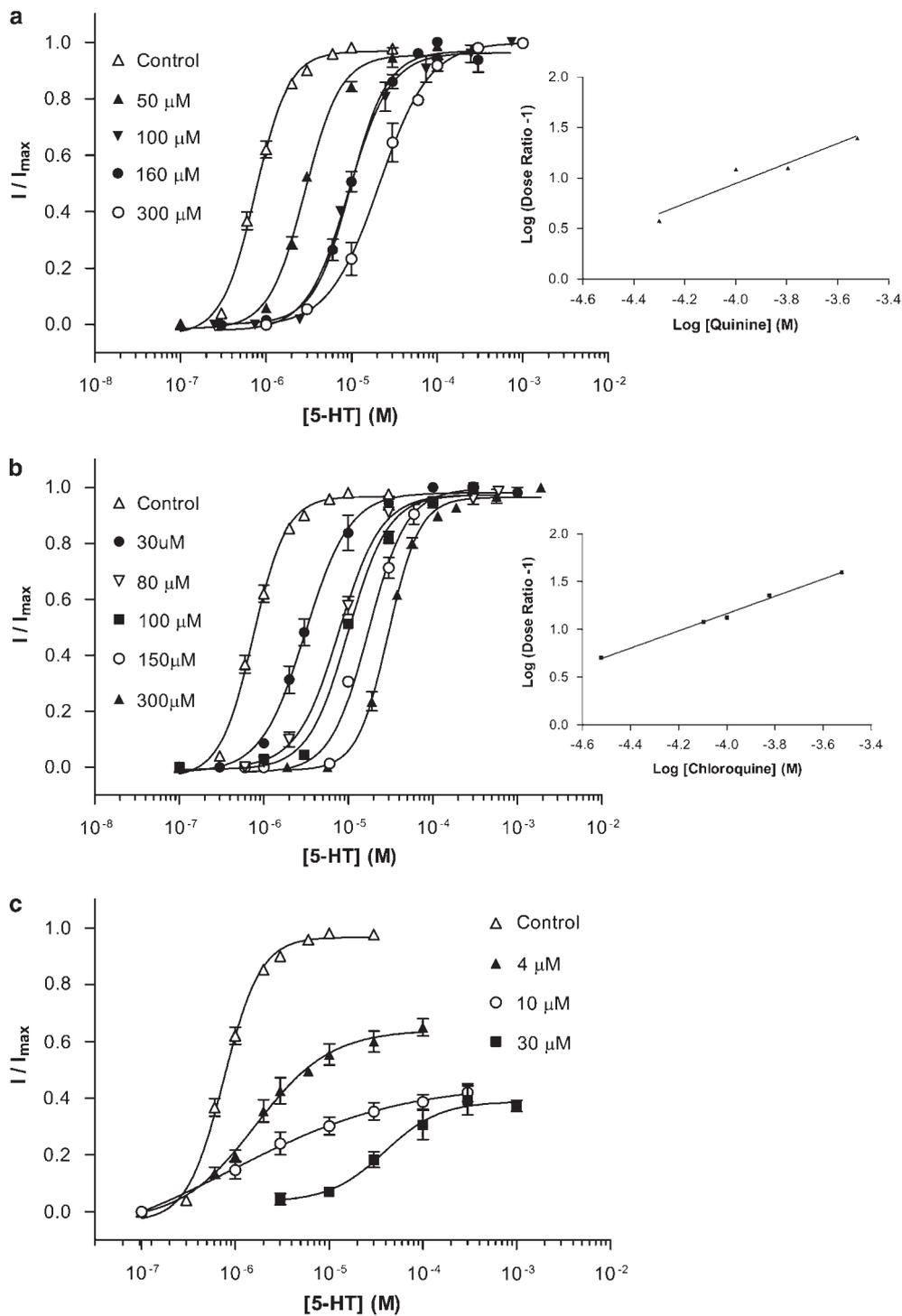
Figure 4 Mechanism of 5-HT$_3$ receptor inhibition by quinine (**a**), chloroquine (**b**) and mefloquine (**c**) in 5-HT$_3$ receptors. Concentration–response curves were performed in the presence or absence of increasing concentrations of antagonist. Parameters derived from these curves can be seen in Table 2. Inset: Schild plots were created from the curves shown, and fitted with Equation 5.

quinine and chloroquine, respectively. The K_B estimates were similar (12.6 and 18.0 μM for quinine and chloroquine, respectively) if data were fitted using nonlinear regression methods (Equation 6) as recommended by Neubig *et al.* (2003) and Lew and Angus (1995). Concentration–response curves in the presence of increasing concentrations of

mefloquine $(4\,\mu\text{M} > 10\,\mu\text{M} > 30\,\mu\text{M})$ displayed concomitant increases in EC$_{50}$, but were not parallel and the maximal responses were reduced, indicating noncompetitive inhibition (Figure 4C). Consistent with these observations, when inhibition of the 6 μM 5-HT response was compared to inhibition of the 0.75 μM response, the IC$_{50}$ values for quinine

Table 2 Parameters derived from 5-HT concentration–response curves in the presence of varying antagonist concentrations

Antagonist (μM)	LogEC$_{50}$ (μM)	EC$_{50}$ (μM)	I$_{max}$/I$_{peak}$	n$_H$	n
Control					
0	−6.12 ± 0.02	0.75	1.00	2.21 ± 0.23	12
Quinine					
50	−5.54 ± 0.03	2.85	0.98	2.07 ± 0.32	3
100	−5.03 ± 0.04	9.26	0.99	1.79 ± 0.28	7
160	−5.01 ± 0.02	9.70	1.00	2.00 ± 0.24	3
300	−4.68 ± 0.02	21.0	1.03	1.47 ± 0.11	8
Chloroquine					
30	−5.42 + 0.01	3.79	1.01	1.55 ± 0.07	4
80	−5.11 + 0.03	7.79	1.01	1.73 ± 0.20	7
100	−5.00 + 0.05	9.99	1.00	1.83 ± 0.36	5
150	−4.76 + 0.07	17.4	1.00	1.91 ± 0.40	3
300	−4.53 + 0.02	29.8	0.99	2.35 ± 0.20	3
Mefloquine					
4	−5.79 ± 0.04	1.64	0.66	1.09 ± 0.11	6
10	−6.05 ± 0.20	0.90	0.47	0.48 ± 0.09	9
30	−4.41 ± 0.08	39.1	0.40	1.47 + 0.40	3

and chloroquine were increased, while the IC$_{50}$ of mefloquine was unaltered (data not shown).

To test whether any of the compounds blocked the channel of the 5-HT$_3$ receptor, experiments were performed at holding potentials of −60 and +40 mV (Figure 5, Table 3). Quinine, chloroquine and mefloquine are positively charged under physiological conditions, and so binding in the channel should be influenced by changes in the membrane holding potential. Comparison of the quinine and chloroquine inhibition curves at −60 and +40 mV showed that they were indistinguishable. For mefloquine there was a rightward shift of the concentration–response curve at +40 mV, indicating that inhibition by this compound was reduced at more positive potentials.

A simple kinetic scheme for binding
The limitations of measuring microscopic rate constants in oocytes is well known, but the experiments described in this study were performed under the same conditions and therefore a comparison of relative rates is valuable (Papke and Thinschmidt, 1998). Inhibition of the 0.75 μM 5-HT response allowed the microscopic rates of association and dissociation for quinine and chloroquine to be determined, and these were found to be well fitted by monoexponential functions (Figure 6; Table 4). The rates were considered to be unaffected by the much slower underlying desensitization of the 5-HT current response (8.16 ± 0.62 s, n = 28). When the reciprocal of these rates was plotted against antagonist concentration, the rates of onset of inhibition (τ_{on}) for both quinine and chloroquine increased linearly with antagonist concentration, while recovery (τ_{off}) was unaltered, as predicted by Equation 7. (Figure 6b and c). Association rates (k_{+1}) were determined from the slope of the $1/\tau_{on}$ curves and dissociation rate constants estimated from the average of the $1/\tau_{off}$ values. The association rates for quinine and chloroquine were 5.6×10^3 and $2.7 \times 10^3 \, M^{-1} s^{-1}$, and the dissocia-

tion rates were 0.09 and $0.10 \, s^{-1}$, yielding dissociation constants of 15.5 and 36.2 μM, respectively (Equation 8). These values are in agreement with a simple kinetic scheme that predicts a single population of antagonist-binding sites with equal affinities; this is consistent with Hill slopes determined from competitive binding with [3H]granisetron, while Hill slopes of the dose–inhibition curves were greater than unity as expected for responses that also have a steep agonist Hill slope, as reported previously (Leff and Dougall, 1993, Fan *et al.*, 1995; Das *et al.*, 2004). Owing to the long preincubation times (>20 s, Figure 2b inset) needed to achieve a stable level of mefloquine inhibition and the poor recovery of the response following the removal of this antagonist, τ_{on} and τ_{off} could not be accurately estimated for this ligand.

Competitive binding using displacement of [3H]granisetron
[3H]Granisetron, at a concentration close to its K_d (1 nM, Figure 7 inset), was displaced in a concentration-dependent manner by all three compounds. IC$_{50}$ values for quinine, chloroquine and mefloquine were similar with values of 30.0 ± 3.5 μM (*n* = 5), 48.5 ± 4.9 μM (*n* = 4) and 71.4 ± 11.4 μM (*n* = 4), respectively. These yielded K_i values of 15.0 μM, 24.2 and 35.7 μM (Equation 2). Hill slopes for quinine, chloroquine and mefloquine were 0.76 ± 0.06, 0.85 ± 0.03 and 1.27 ± 0.09.

Docking studies
Docking quinine and chloroquine into the 5-HT$_3$ receptor-binding site yielded a series of docking solutions for each antagonist. These were split into groups based on the orientation of the ligand and GOLD scores (Olsen *et al.*, 2004). Docking of mefloquine was not performed as this ligand displayed a mixed competitive/noncompetitive behaviour.

The results of quinine docking fell into two alternative groups designated A and B. In solution A (Figure 8a), the tertiary ammonium group of quinine was located between the aromatic rings of Y234 and W183, and the quinoline ring was orientated towards the membrane. The distances between the nitrogen atom of the ammonium group and the centroids of the aromatic rings of Y234 and W183 were between 4 and 5 Å, which is ideal for a cation–π interaction. There is a potential hydrogen bond between the hydroxyl group of quinine and the carboxylate group of the E129 side chain. In solution B (Figure 8b), the quinoline ring projected in the opposite direction towards loop E, although the tertiary ammonium group remains between Y234 and W183 and still has the potential to form a cation–π interaction. In this orientation there were a series of potential hydrogen bonds between the hydroxyl group of quinine and the hydroxyl group of Y143 and backbone carbonyl oxygen of W183, in addition to a hydrogen bond formed between the quinoline nitrogen and the primary amide of Q151.

Docking of chloroquine yielded solutions that also fell into two main groups designated C and D. Both solutions placed the quinoline ring between the aromatic rings of W183 and Y234. The centroid–centroid distances between
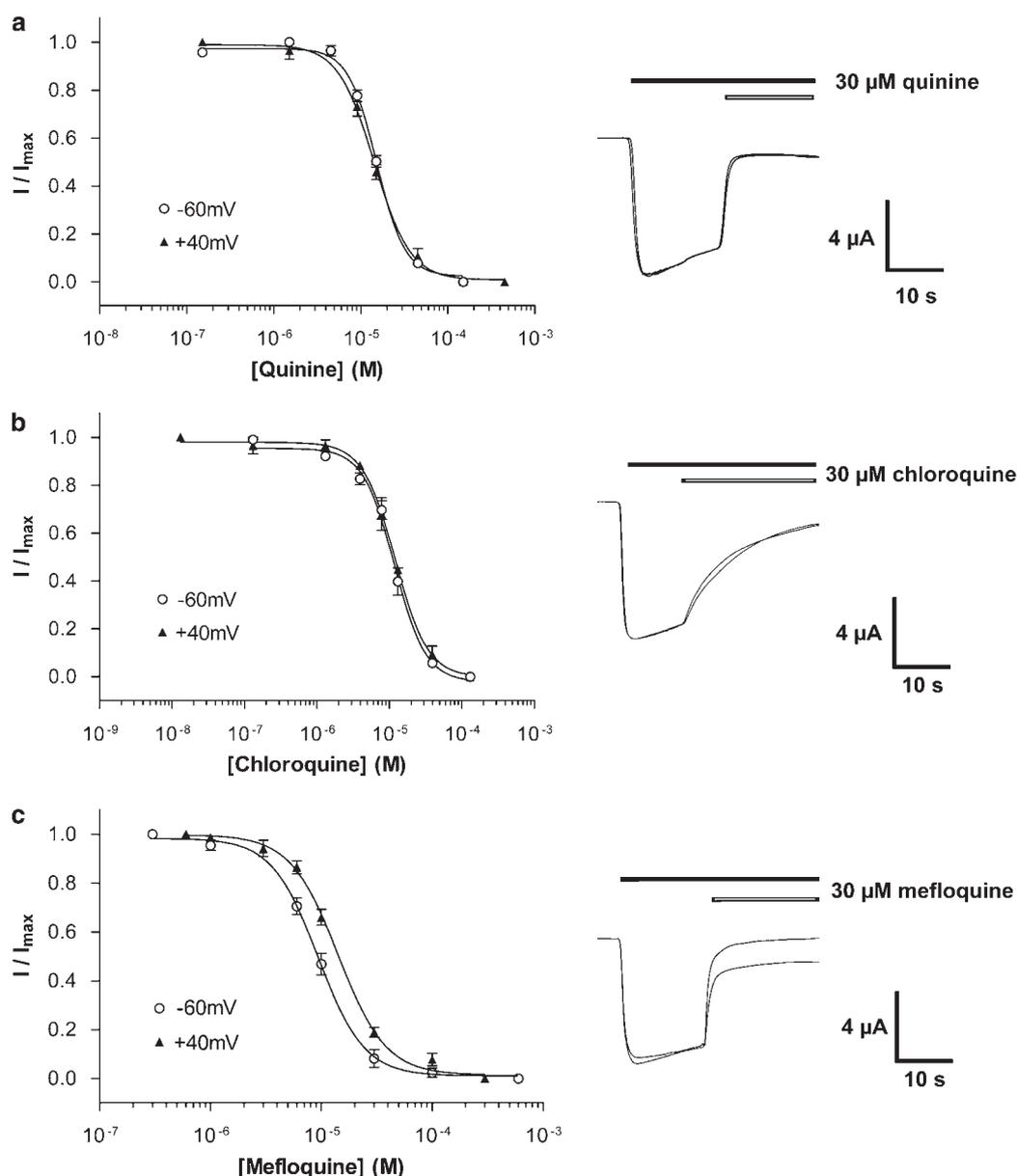
Figure 5 Voltage sensitivity of antagonist block at the 5-HT₃ receptor. Inhibition of the $0.75\,\mu M$ 5-HT response was performed at either $-60\,mV$ or $+40\,mV$ for quinine (**a**), chloroquine (**b**) and mefloquine (**c**). Responses were normalized to the peak response for each oocyte and are shown as the mean±s.e.m. for a series of experiments. Parameters derived from these curves can be seen in Table 3. Quinine and chloroquine were co-applied. Mefloquine was pre-applied for 25 s and was immediately followed by co-application with 5-HT. To the right of each curve, representative examples of scaled responses are shown for the application of 5-HT ($6\,\mu M$, filled bar) and antagonist (open bar). The antagonist concentration used to inhibit the response is shown next to each trace. It can be seen that the inhibitory effects of quinine and chloroquine are comparable at the two potentials, while mefloquine displayed reduced inhibition at $+40\,mV$.

the ring planes were within 5 Å, suggesting a possible π–π interaction. In model C (Figure 8c), the tertiary ammonium was orientated towards the membrane and indicated the possibility of a cation-π interaction with the aromatic ring of F226. In solution D, the tertiary ammonium of chloroquine was orientated away from the membrane, which would enable the formation of a hydrogen bond between the tertiary ammonium and the hydroxyl group of Y234, as well as a hydrogen bond between the secondary amine of chloroquine and the hydroxyl group of Y143 (Figure 8d).

Discussion

The antimalarial compounds quinine, chloroquine and mefloquine have structural similarity to 5-HT₃ receptor antagonists. Here, we show that all three compounds inhibit 5-HT₃ receptor-mediated responses and binding of the competitive radiolabelled antagonist [³H]granisetron at micromolar concentrations. Quinine and chloroquine inhibit 5-HT₃ responses in a manner that is consistent with competitive inhibition, while the characteristic of mefloquine inhibition is predominantly channel block.

Table 3 Voltage sensitivity of inhibition

Antagonist	log IC₅₀ (μM)	IC₅₀ (μM)	nH	n
Quinine				
−60mV	−4.87±0.02	13.4	−2.09±0.21	12
+40mV	−4.82±0.02	15.2	−2.66±0.31	3
Chloroquine				
−60mV	−4.93±0.02	11.8	−1.90±0.39	14
+40mV	−4.92±0.01	12.0	−1.93±0.09	3
Mefloquine				
−60mV	−5.03±0.02	9.36	−2.08±0.18	13
+40mV	−4.85±0.02	14.2	−2.01±0.17	6

Table 4 Inhibition and recovery of responses to 5-HT (0.75 μM) in the presence of quinine or chloroquine

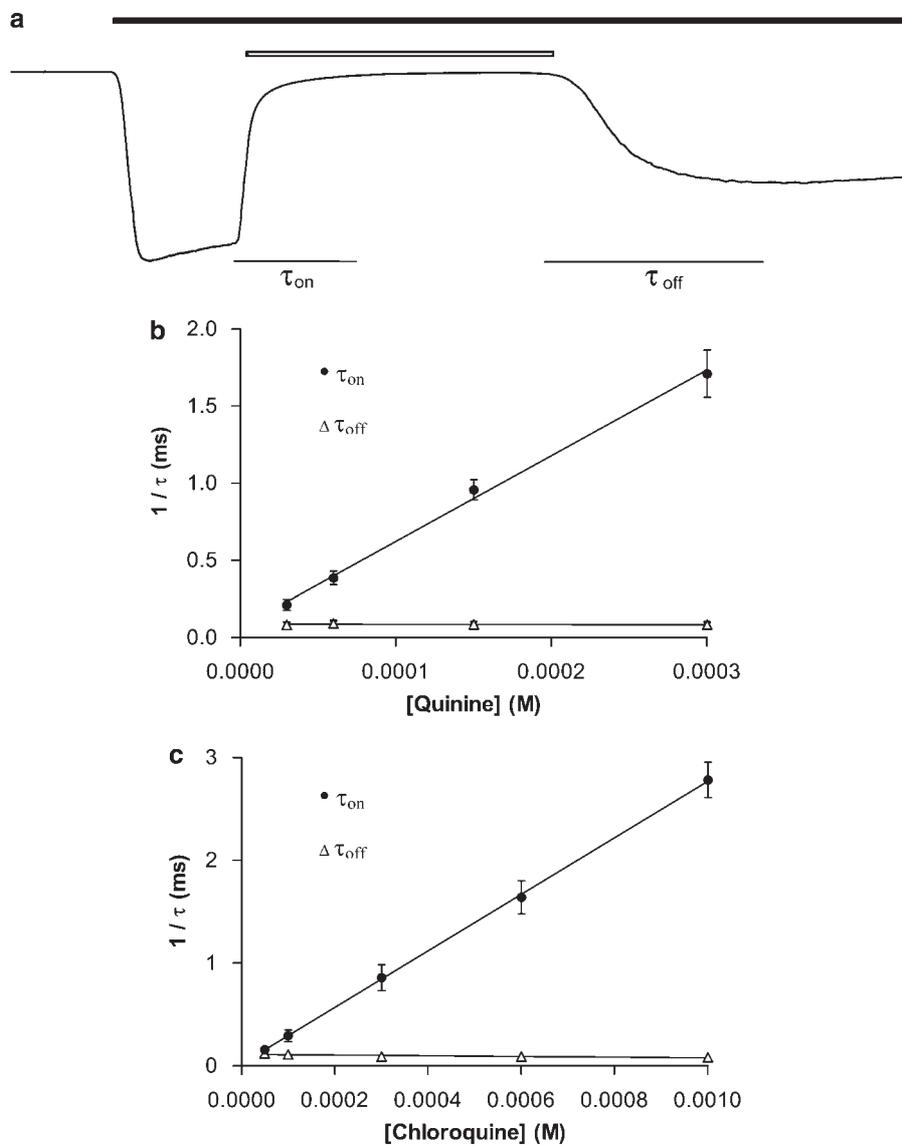| Antagonist μM	τ_{on} (ms)	τ_{off} (ms)	n
Quinine			
30	4.71±0.65	12.10±0.63	11
60	2.59±0.25	10.89±0.95	9
150	1.04±0.06	11.56±1.06	8
300	0.58±0.04	11.95±0.79	11
Chloroquine			
50	6.30±0.38	8.21±0.62	12
100	3.41±0.31	9.07±0.37	11
300	1.16±0.12	10.87±0.52	11
600	0.61±0.06	10.89±0.54	11
1000	0.36±0.02	12.07±0.47	10

Figure 6 Kinetics of quinine and chloroquine interactions at the 5-HT₃ receptor. (**a**) A sample trace showing the onset (τ_{on}) and recovery (τ_{off}) of antagonist inhibition (open bar) during a 5-HT application (filled bar). Association and dissociation constants for inhibition by quinine (**b**) and chloroquine (**c**) were well fitted by monoexponential functions and these values can be seen in Table 4. A plot of the reciprocal rate constant versus antagonist concentration shows that for both quinine and chloroquine the association rate changed linearly with concentration, while the dissociation rate did not alter significantly.

The observation that quinine and chloroquine competitively inhibit receptor responses was anticipated, as there are structural similarities between these compounds and 5-HT₃
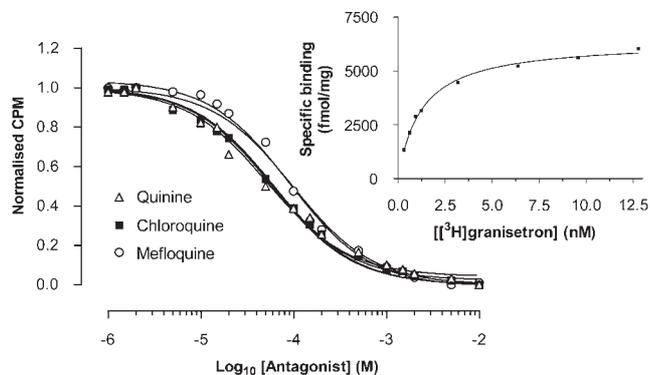

Figure 7 Competition binding curves for the displacement of 1 nM [³H]granisetron by varying concentrations of quinine, chloroquine and mefloquine in transiently transfected HEK-293 cells expressing 5-HT₃ receptors. Each curve is from a single experiment, but is representative of at least four other similar curves. Data were normalized to [³H]granisetron binding in the absence of antagonist and fitted with Equation 1. Inset shows a typical binding curve for [³H]granisetron alone.

pharmacophore models. We explored the potential interactions of these two compounds with the amino acids that constitute the 5-HT₃ receptor ligand-binding site by docking these ligands into the binding pocket. We successfully docked quinine with its tertiary amine located between W183 and Y234. This is also where we believe the primary amine of bound 5-HT is located (Reeves *et al.*, 2003). W183 is known to form a cation-π interaction with bound 5-HT and the tertiary amine of quinine could form a similar interaction. There is strong evidence that an aromatic residue is required at position 234 in the 5-HT₃ receptor, and at the equivalent location (Y198) in the nACh receptor; indeed, the aromatic nature of this location is conserved in almost all the subunits of this superfamily (Kearney *et al.*, 1996; Beene *et al.*, 2004; Price and Lummis, 2004). The location of the quinoline ring was not as easy to distinguish as two possible orientations were suggested (Figure 8a and b). Currently we favour solution 8a, where the carboxylate group of Glu129 forms an H bond with the hydroxyl group of quinine. Glu129 is a critical binding residue for the antagonist granisetron, and in this position quinine is similarly orientated to the preferred orientation of granisetron in the 5-HT-binding site (Thompson *et al.*, 2005, 2006a; Sullivan
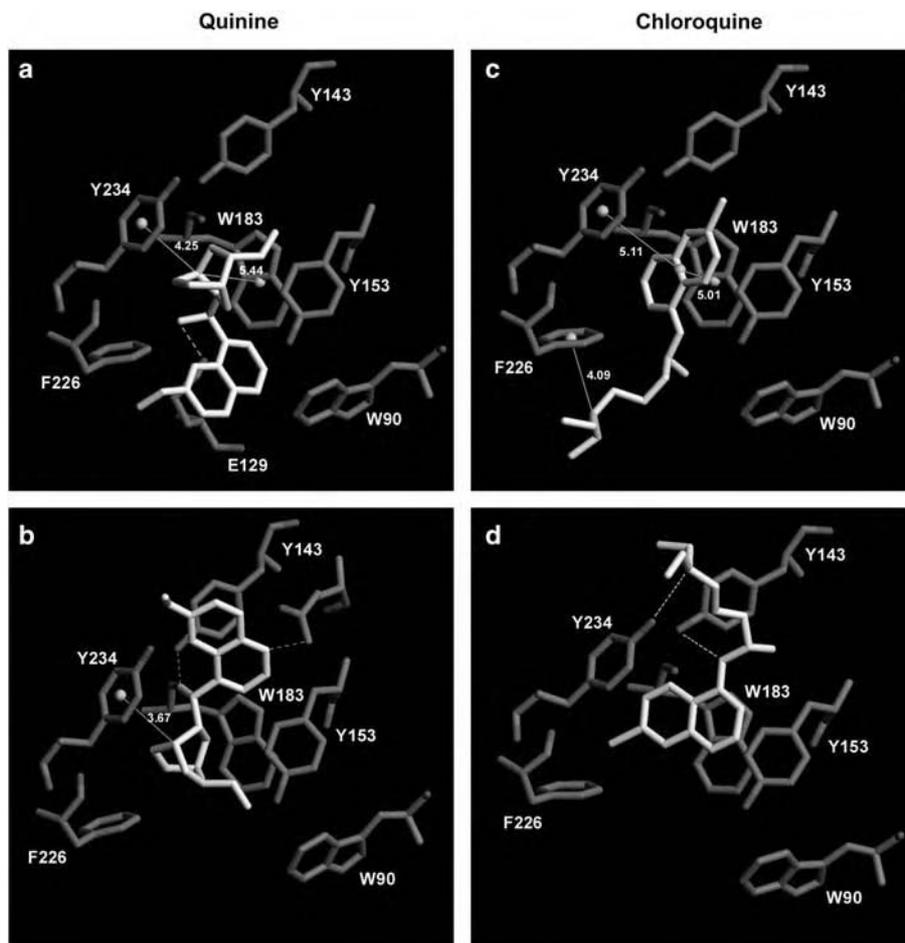

Figure 8 Representative examples of the docked ligands showing the orientation of the main residues that define these models. Quinine (**a** and **b**) and chloroquine (**c** and **d**) are shown in white in the centre of each image. Solid lines show distances between the ligands and the amino-acid residues described in the text. Dashed lines indicate potential hydrogen bonds, and are also described in the text.

et al., 2006). Docking of chloroquine revealed two orientations that were distinct from docked quinine, as the quinoline ring of chloroquine was located between W183 and Y234, suggesting a possible π–π interaction (Figure 8c and d). A potential cation-π interaction was detected between F226 and the tertiary ammonium of chloroquine. Because of this and the similarities in orientation with quinine and previous docking studies of granisetron, we believe that solution 8d may reflect the true binding orientation. It is interesting to note that the aromatic side chains of W183 and Y234 prefer a π-cation interaction with the tertiary ammonium of quinine where as the quinoline ring of chloroquine forms a π–π sandwich with W183 and Y234. This difference may be the consequence of steric restrictions within the binding site, as chloroquine has a long and flexible side chain that can adopt many different conformations while quinine has a more bulky and rigid azabicyclic ring.

Mefloquine does not appear to be a competitive inhibitor at the 5-HT₃ receptor, despite its similarities with 5-HT₃ pharmacophore models and the structural features it shares with quinine and chloroquine. Our evidence suggests it inhibits the 5-HT-mediated current by blocking the 5-HT₃ receptor channel. Firstly, concentration–response curves in the presence of increasing concentrations of mefloquine showed that the effect of the antagonist was not surmountable. Secondly, inhibition was increased by preincubation with mefloquine, suggesting an action at the closed channel. Finally, the inhibition curve at $+40$ mV was shifted to the right when compared to that at -60 mV, indicating voltage dependence. The simplest explanation for this voltage dependence is the impairment of ion flow by channel block. Given the small difference in IC₅₀ values recorded at the two potentials, it is likely that mefloquine binds at a shallow position in the channel or within the outer vestibule as has been suggested for channel blockers of the nACh receptor (Tikhonov *et al.*, 2004).

Interestingly, mefloquine was able to displace specific [³H]granisetron binding, although at higher concentrations than required for its channel blocking activity. This is similar to previous studies of diltiazem and verapamil which block the 5-HT₃ receptor pore, but also displace [³H]granisetron binding at higher concentrations (Hargreaves *et al.*, 1996; Gunthorpe and Lummis, 1999). Our results indicate that at higher concentrations mefloquine may have a mixed competitive/noncompetitive behaviour, similar to the actions of quinine and quinidine at $\alpha9\alpha10$ nACh receptors, and to the proposed effects of 5-hydroxyindole at the 5-HT₃ receptor (Kooyman *et al.*, 1993; Ballestero *et al.*, 2005). Similar effects on the 5-HT₃ receptor current have also been observed for the antihypertensive drug ifenprodil and the antipsychotic, flupentixol. At concentrations similar to those used here, inhibition of the 5-HT-induced response by ifenprodil was reversible, enhanced by pre-application and was noncompetitive (McCool and Lovinger, 1995; Barann *et al.*, 1998). Inhibition by flupentixol was also reversible, enhanced by pre-application, was noncompetitive and was characterized by the appearance of 'tail currents' when the drug was removed (Rammes *et al.*, 2004).

The effects of quinine and chloroquine on other members of the Cys-loop family have been reported previously,

although the mode of action of the compounds appears to vary. At similar concentrations to those reported here, quinine acted as a channel blocker at muscle-type ACh channels and inhibited [¹²⁵I]α-bungarotoxin binding at concentrations higher than those required for the channel effects (Hargreaves *et al.*, 1996; Sieb *et al.*, 1996). At $\alpha9\alpha10$ nACh receptors, quinine and chloroquine appear more potent with reported IC₅₀ values of 0.97 and 0.39 μM, respectively, and a mixed competitive/noncompetitive behaviour was reported (Sieb *et al.*, 1996; Ballestero *et al.*, 2005). In humans, the blood concentration of mefloquine required to be 99% effective at reducing *Plasmodium falciparum* infection has been reported as 2.2 and 4.1 μM (Lobel *et al.*, 1993; Ramharter *et al.*, 2004). For chloroquine, 99% efficiency is achieved at 44.4 μM and for quinine it is 1.57 μM (Ramharter *et al.*, 2004). For chloroquine and mefloquine these concentrations are close to the IC₅₀ concentrations at both 5-HT₃ and nACh receptors.

In summary, we have used a combination of electrophysiology, ligand binding, homology modelling and simulated docking to define the mechanisms by which quinine, chloroquine and mefloquine inhibit the 5-HT₃ receptor response. Our observations further extend the number of receptors known to be affected by these compounds and the growing diversity of targets may account for the broad spectrum of side effects that have been reported by patients receiving them (Luzzi and Peto, 1993; Palmer *et al.*, 1993; Taylor and White, 2004). Inhibition of the 5-HT₃-mediated current could have wide-ranging effects in the nervous system, as 5-HT₃ receptors can modulate a variety of neurotransmitter responses such as those to GABA, dopamine and cholecystokinin (Thompson *et al.*, 2006b).

Acknowledgements

Conflict of interest

The authors state no conflict of interest.

References

Arunlakshana O, Schild HO (1959). Some quantitative uses of drug antagonists. *Br J Pharmacol Chemother* **14**: 48–58.

Ballestero JA, Plazas PV, Kracun S, Gomez-Casati ME, Taranda J, Rothlin CV *et al.* (2005). Effects of quinine, quinidine and chloroquine on $\alpha9$ $\alpha10$ nicotinic cholinergic receptors. *Mol Pharmacol* **68**: 822–829.

Barann M, Bonisch H, Urban BW, Gothert M (1998). Inhibition of 5-HT₃ receptor cation channels by ifenprodil in excised patches of N1E-115 cells. *Naunyn Schmiedebergs Arch Pharmacol* **358**: 145–152.

Antimalarial drugs inhibit 5-HT$_3$ receptors
AJ Thompson *et al*
677

Beene DL, Price KL, Lester HA, Dougherty DA, Lummis SC (2004). Tyrosine residues that control binding and gating in the 5-hydroxytryptamine$_3$ receptor revealed by unnatural amino acid mutagenesis. *J Neurosci* **24**: 9097–9104.

Bray PG, Martin RE, Tilley L, Ward SA, Kirk K, Fidock DA (2005). Defining the role of PfCRT in *Plasmodium falciparum* chloroquine resistance. *Mol Microbiol* **56**: 323–333.

Das P, Bell-Horner CL, Huang RQ, Raut A, Gonzales EB, Chen ZL *et al.* (2004). Inhibition of type A GABA receptors by L-type calcium channel blockers. *Neuroscience* **124**: 195–206.

Davies PA, Pistis M, Hanna MC, Peters JA, Lambert JJ, Hales irkness TG *et al.* (1999). The 5-HT$_{3B}$ subunit is a major determinant of serotonin-receptor function. *Nature* **397**: 359–363.

Fan P, Oz M, Zhang L, Weight FF (1995). Effect of cocaine on the 5-HT$_3$ receptor-mediated ion current in *Xenopus* oocytes. *Brain Res* **673**: 181–184.

Goldin LR (1992). Maintenance of *Xenopus laevis* and Oocyte Injection. In: Bernardo R, Iverson LE (eds.) *Methods in Enzymology.* Academic Press: New York, **vol. 207** pp 267–279.

Gunthorpe MJ, Lummis SC (1999). Diltiazem causes open channel block of recombinant 5-HT$_3$ receptors. *J Physiol* **519**: 713–722.

Hargreaves AC, Gunthorpe MJ, Taylor CW, Lummis SC (1996). Direct inhibition of 5-hydroxytryptamine$_3$ receptors by antagonists of L-type Ca^{2+} channels. *Mol Pharmacol* **50**: 1284–1294.

Jordan M, Schallhorn A, Wurm FM (1996). Transfecting mammalian cells: optimization of critical parameters affecting calcium-phosphate precipitate formation. *Nucleic Acids Res* **24**: 596–601.

Kearney PC, Nowak MW, Zhong W, Silverman SK, Lester HA, Dougherty DA (1996). Dose–response relations for unnatural amino acids at the agonist binding site of the nicotinic acetylcholine receptor: tests with novel side chains and with several agonists. *Mol Pharmacol* **50**: 1401–1412.

Kooyman AR, van Hooft JA, Vijverberg HP (1993). 5-Hydroxyindole slows desensitization of the 5-HT$_3$ receptor-mediated ion current in N1E-115 neuroblastoma cells. *Br J Pharmacol* **108**: 287–289.

Leff P, Dougall IG (1993). Further concerns over Cheng–Prusoff analysis. *Trends Pharmacol Sci* **14**: 110–112.

Lew MJ, Angus JA (1995). Analysis of competitive agonist–antagonist interactions by nonlinear regression. *Trends Pharmacol Sci* **16**: 328–337.

Liman ER, Tytgat J, Hess P (1992). Subunit stoichiometry of a mammalian K$^+$ channel determined by construction of multimeric cDNAs. *Neuron* **9**: 861–871.

Lobel HO, Miani M, Eng T, Bernard KW, Hightower AW, Campbell CC (1993). Long-term malaria prophylaxis with weekly mefloquine. *Lancet* **341**: 848–851.

Lummis SC, Sepulveda MI, Kilpatrick GJ, Baker J (1993). Characterization of [^{3}H] meta-chlorophenylbiguanide binding to 5-HT$_3$ receptors in N1E-115 neuroblastoma cells. *Eur J Pharmacol* **243**: 7–11.

Luzzi GA, Peto TE (1993). Adverse effects of antimalarials. *An update Drug Saf* **8**: 295–311.

McCool BA, Lovinger DM (1995). Ifenprodil inhibition of the 5-hydroxytryptamine$_3$ receptor. *Neuropharmacology* **34**: 621–629.

Neubig RR, Spedding M, Kenakin T, Christopoulos A (2003). International Union of Pharmacology Committee on Receptor Nomenclature and Drug Classification. XXXVIII. Update on terms and symbols in quantitative pharmacology. *Pharmacol Rev* **55**: 597–606.

Niesler B, Frank B, Kapeller J, Rappold GA (2003). Cloning, physical mapping and expression analysis of the human 5-HT$_3$ serotonin receptor-like genes HTR3C, HTR3D and HTR3E. *Gene* **310**: 101–111.

Olsen L, Pettersson I, Hemmingsen L, Adolph HW, Jorgensen FS (2004). Docking and scoring of metallo-beta-lactamases inhibitors. *J Comput Aided Mol Des* **18**: 287–302.

Palmer KJ, Holliday SM, Brogden RN (1993). Mefloquine. A review of its antimalarial activity, pharmacokinetic properties and therapeutic efficacy. *Drugs* **45**: 430–475.

Papke RL, Thinschmidt JS (1998). The correction of alpha7 nicotinic acetylcholine receptor concentration–response relationships in *Xenopus* oocytes. *Neurosci Lett* **256**: 163–166.

Price KL, Lummis SC (2004). The role of tyrosine residues in the extracellular domain of the 5-hydroxytryptamine$_3$ receptor. *J Biol Chem* **279**: 23294–23301.

Ramharter M, Wernsdorfer WH, Kremsner PG (2004). *In vitro* activity of quinolines against *Plasmodium falciparum* in Gabon. *Acta Trop* **90**: 55–60.

Rammes G, Eisensamer B, Ferrari U, Shapa M, Gimpl G, Gilling K *et al.* (2004). Antipsychotic drugs antagonize human serotonin type 3 receptor currents in a noncompetitive manner. *Mol Psychiatry* **9**: 846–858.

Reeves DC, Lummis SC (2002). The molecular basis of the structure and function of the 5-HT$_3$ receptor: a model ligand-gated ion channel (review). *Mol Membr Biol* **19**: 11–26.

Reeves DC, Sayed MF, Chau PL, Price KL, Lummis SC (2003). Prediction of 5-HT$_3$ receptor agonist-binding residues using homology modeling. *Biophys J* **84**: 2338–2344.

Sali A, Blundell TL (1993). Comparative protein modelling by satisfaction of spatial restraints. *J Mol Biol* **234**: 779–815.

Shi J, Blundell TL, Mizuguchi K (2001). FUGUE: sequence-structure homology recognition using environment-specific substitution tables and structure-dependent gap penalties. *J Mol Biol* **310**: 243–257.

Sieb JP, Milone M, Engel AG (1996). Effects of the quinoline derivatives quinine, quinidine, and chloroquine on neuromuscular transmission. *Brain Res* **712**: 179–189.

Sullivan NL, Thompson AJ, Price K, Lummis SCR (2006). Defining the roles of Asn-128, Glu-129 and Phe-130 in loop A of the 5-HT$_3$ receptor. *Mol Memb Biol* **23**: 1–10.

Taylor WR, White NJ (2004). Antimalarial drug toxicity: a review. *Drug Saf* **27**: 25–61.

Thompson AJ, Padgett CL, Lummis SC (2006a). Mutagenesis and molecular modeling reveal the importance of the 5-HT$_3$ receptor F-loop. *J Biol Chem* **281**: 16576–16582.

Thompson AJ, Zhang L, Lummis SCRL (2006b). The 5-HT$_3$ Receptor. In: Roth B (ed.) *The serotonin receptors: from molecular pharmacology to human therapeutics* pp 439–457.

Thompson AJ, Price KL, Reeves DC, Chan SL, Chau PL, Lummis SC (2005). Locating an antagonist in the 5-HT$_3$ receptor binding site using modeling and radioligand binding. *J Biol Chem* **280**: 20476–20482.

Tikhonov DB, Mellor IR, Usherwood PN (2004). Modeling non-competitive antagonism of a nicotinic acetylcholine receptor. *Biophys J* **87**: 159–170.

Uhlemann A, Yuthavong Y, Fidock DA (2005). Mechanisms of Antimalarial Drug Action and Resistance. Sherman IW (ed.) *Molecular Approaches to Malaria.* ASM Press: Washington, USA, pp 429–461.